BUTP-95/7
NORDITA 95/41 N,P
hep-ph/9505348

Mass of scalar resonances beyond the large-N_c limit*

C. Bruno[†‡]
Institute for Theoretical Physics, University of Bern,
Sidlerstrasse 5, CH-3012 Bern, Switzerland

and

E. Pallante[§]
NORDITA, Blegdamsvej 17, 2100 Copenhagen, Denmark

Abstract

Within the Extended Nambu Jona-Lasinio model we analyse the $1/N_c$-corrections to the leading order result $M_S = 2M_Q$ where M_Q is the constituent quark mass.

BUTP-95/7
NORDITA 95/41 N,P
May 1995

*Work supported in part by the EEC Human Capital and Mobility Program

† email: cbruno@butp.unibe.ch

‡also at: INFN-Laboratori Nazionali di Frascati P.O. Box 13, I-00044 Frascati, Italy

§ email: pallante@nbivax.nbi.dk

Effective constituent quark models *à la* Nambu Jona-Lasinio have recently been used to a large extent to describe the low-energy behaviour of QCD and the hadron spectrum (see [1] for a recent review). Phenomenologically these models are found to be very successful in reproducing the experimental values of the low-energy coupling constants to $O(p^4)$ in Chiral Perturbation Theory (χPT) [2]. Many of the couplings between resonances and pseudoscalar mesons have also been computed [2, 3] and compare well with experiment, as well as the vector and axial-vector masses [2, 4].

When we turn our attention to the scalar sector the situation is less satisfactory. Within the Extended Nambu Jona-Lasinio (ENJL) model the scalar two-point function shows up a pole at a mass $M_S = 2M_Q$ [4], where M_Q is the constituent quark mass. With a typical value of $M_Q = 250 \div 350$ MeV (this range of values is taken from the different fits of [2]) one has $M_S = 500 \div 700$ MeV. Experimentally there is no evidence for so low a scalar resonance. Until 1976 the Particle Data Book quoted a scalar resonance (called ϵ) between 600 and 800 MeV with a width of more than 600 MeV. Because of this very large width it has then been discarded from the particle tables. Unclear experimental signal of a narrow scalar state around 750 MeV is reported in [5], while the first clear scalar resonances are the $a_0(983)$ and the isosinglet $f_0(975)$ states. The proper $q\bar{q}$ assignment of the $a_0(983)$ remains a problem. Its interpretation as ordinary $q\bar{q}$ system [6] is not excluded; other possible interpretations are as a $q\bar{q}q\bar{q}$ state [7] or a $K\bar{K}$ bound state [8]. For the $f_0(975)$ the analysis of ref. [9] supports the prediction of the unitarized quark model which interprets $f_0(975)$ as a $q\bar{q}$ resonance with a large admixture of $K\bar{K}$ virtual state, while ref. [10] almost excludes its interpretation as a $K\bar{K}$ molecule and favours a conventional Breit-Wigner-like structure. In both cases the interpretation of the $f_0(975)$ as an ordinary $q\bar{q}$ state is almost excluded. Recently, a fit of the available data has been performed [11] indicating that the $K\bar{K}$ component is large for both the $a_0(983)$ and $f_0(975)$ states.

In the large-N_c limit of the ENJL model the isoscalar resonance situated at $2M_Q$ is predicted to have a very large width of more than 600 MeV [12]. Assuming that such a resonance exists, qualitatively at least, there would be no surprise if $1/N_c$-corrections in relation to the large isoscalar width created a non-degeneracy between the isoscalar (the hypothetical ϵ) and the scalar octet (which could be the a_0).

This is the physical intuition we would like to precise. The framework of the ENJL model offers a starting point to study the $1/N_c$-corrections. At this point it is worth mentioning that the NJL-like models contain most of the effective low-energy

models discussed in the literature as particular cases. Therefore such an approach lies in a quite general context.

The effective ENJL Lagrangian is given by [2]:

$$\mathcal{L}_{ENJL} = \mathcal{L}_{QCD}^{\Lambda_\chi} + \frac{8\pi^2 G_S}{N_c \Lambda_\chi^2}[(\bar{q}q)^2 - (\bar{q}\gamma_5 q)^2] - \frac{8\pi^2 G_V}{N_c \Lambda_\chi^2}[(\bar{q}\gamma_\mu q)^2 - (\bar{q}\gamma_\mu\gamma_5 q)^2]. \qquad (1)$$

The problem of the connection between QCD and this Lagrangian has been addressed in [2]. The Lagrangian (1) is the first term of a double expansion in $1/N_c$ and in $1/\Lambda_\chi^2$, $\Lambda_\chi \simeq 1$ GeV being the ultraviolet cutoff of the low-energy effective theory.

The effective action derived in [2] from the Lagrangian (1) is subject to two types of $1/N_c$ corrections. The first type will not be studied here. It concerns the $1/N_c$ expansion mentioned above: at next-to-leading order in $1/N_c$, there are other dimension six fermionic operators compatible with the symmetries of the original QCD Lagrangian. The second type appears when one considers loops made of chains of quark bubbles, *i.e.* loops of mesons. In this article we shall be interested in the latter.

In section 1 we explain the relation between the quark-bubbles resummation in the non-bosonized ENJL model and the bosonized version. Then, in section 2 we present the effective Lagrangian we shall use in order to perform the loop calculation. The coupling constants of this Lagrangian are derived within the ENJL model. Section 3 deals with the analysis of the $1/N_c$-corrections. We show the corrections to the gap-equation, the mass-splitting between the scalar singlet and non-singlet, and the overall shift of the singlet. Finally section 4 is devoted to conclusions and remarks.

1 Bosonized versus non-bosonized version of the ENJL model.

Let us consider the isoscalar two-point function $\Pi(q^2) = i \int d^4x\ e^{iqx} \langle 0|TS(x)S(0)|0\rangle$ where $S(x) \equiv -\frac{1}{\sqrt{2}}\bar{q}(x)q(x)$. This Green function has been computed in the large-N_c limit within the non-bosonized version of the ENJL model using proper-time regularization with an ultra-violet cut-off Λ_χ. The result [4] is obtained by resumming the geometrical series

$$\Pi(Q^2)^{(N_c\to\infty)} = \bar{\Pi}(Q^2)\sum_{n=0}^{\infty}\Big(g_S\bar{\Pi}(Q^2)\Big)^n, \tag{2}$$

where

$$\bar{\Pi}(Q^2) = \frac{1}{g_S} - (Q^2+(2M_Q)^2)Z_S(Q^2) \tag{3}$$

is the bare fermion loop diagram in the mean-field approximation, $Z_S(Q^2)$ is the wave function renormalization constant

$$Z_S(Q^2) = \frac{N_c}{16\pi^2}2\int_0^1 d\alpha\Gamma\Big(0,\frac{\alpha(1-\alpha)Q^2+M_Q^2}{\Lambda_\chi^2}\Big) \tag{4}$$

with $\Gamma(0,\epsilon) = \int_\epsilon^\infty dz\frac{1}{z}e^{-z}$ and $g_S = 4\pi^2G_S/N_c\Lambda_\chi^2$. One obtains

$$\Pi(Q^2)^{(N_c\to\infty)} = \frac{\bar{\Pi}(Q^2)}{1-g_S\bar{\Pi}(Q^2)} = -\frac{1}{g_S}\left(1-\frac{(Z_S(Q^2)g_S)^{-1}}{Q^2+(2M_Q)^2}\right). \tag{5}$$

The next-to-leading contribution in $1/N_c$ is built by dressing the leading-N_c scalar two-point function with one loop of linear chains of constituent quark bubbles. We shall concentrate here on the example of the self-energy diagram, as shown in Fig.1, involving only the isoscalar coupling g_S.

These multiloop diagrams contain overlapping divergences. The regularization procedure we use is as follows: first we regularize the momenta running in the quark-bubbles and secondly we regularize the remaining momentum which runs in the internal loop made of quark-bubbles. This allows us to use the expressions found in [4] for the two-point functions, like Eq. (5). The divergences occurring in the loop calculation have to be interpreted as physical divergences since the ENJL model is an effective non-renormalizable theory in which all the momenta are cutoff at the ultra-violet scale Λ_χ.

Notice also that expressions like (5) should not be used beyond the convergence radius of the geometrical series, given in this case by $q^2 = -Q^2 = (2M_Q)^2$. Since $2M_Q$ is of the order of Λ_χ it is legitimate to make the integration over the internal loop, *i.e.* the bosonic loop, up to such energies.

In order to compute the self-energy diagram of Fig. 1 we need the three-point function

$$\bar{T}(q,k) = \int d^4x\ d^4y\ e^{iqx} e^{iqy} \langle 0|TS(x)S(y)S(0)|0\rangle. \tag{6}$$

It is found to be

$$\bar{T}(q,k) = \frac{N_c}{16\pi^2} 4M_Q \Big[\Gamma\Big(0, \frac{M_Q^2}{\Lambda_\chi^2}\Big) - \frac{2}{3}\Gamma\Big(1, \frac{M_Q^2}{\Lambda_\chi^2}\Big)\Big] + O(k^2, q^2, (q-k)^2). \tag{7}$$

We now proceed to the resummation $g_S\Pi = \frac{g_S\bar{\Pi}}{1-g_S\bar{\Pi}} + \frac{1}{1-g_S\bar{\Pi}} g_s\Sigma \frac{1}{1-g_S\bar{\Pi}} + \cdots$ and get

$$\Pi(Q^2) = -\frac{1}{g_S}\left(1 - \frac{(Z_S(Q^2)g_S)^{-1}}{Q^2 + (2M_Q)^2 - \Sigma(Q^2)Z_S(Q^2)^{-1}}\right), \tag{8}$$

with

$$\Sigma(q^2) = \frac{1}{2} g_S^2 \int \frac{d^4k}{(2\pi)^4} \bar{T}(q,k)^2 \frac{1}{1 - g_S\bar{\Pi}(k^2)} \frac{1}{1 - g_S\bar{\Pi}((q-k)^2)}. \tag{9}$$

This expression has to be compared with the one obtained within the bosonized approach, where we consider the three-scalars vertex at lowest order in the derivative expansion with coupling λ:

$$\Pi(Q^2) = -\frac{1}{g_S}\left(1 - \frac{(Z_S(0)g_S)^{-1}}{Q^2 + (2M_Q)^2 - \lambda^2\, I(Q^2)}\right), \tag{10}$$

where

$$I(q^2) = \frac{1}{2} \int \frac{d^4k}{(2\pi)^4} \frac{1}{k^2 - (2M_Q)^2} \frac{1}{(q-k)^2 - (2M_Q)^2}. \tag{11}$$

Considering now Eqs. (9) and (8) and substituting $\bar{T}(q,k)$ with $\bar{T}(0,0)$ and $Z_S(Q^2)$ with $Z_S(0)$, Eq. (8) reduces to Eq. (10) with

$$\lambda = \frac{\bar{T}(0,0)}{Z_S(0)^{3/2}}. \tag{12}$$

This is nothing but the expression of the three-scalars vertex coupling $\lambda_3/3!$ which is obtained in the next section (Eq. 15), within the effective action approach [¶]. Numerically the error made in approximating $T(q,k)$ with $T(q,0)$ is of the order of thirty percent when k^2 is below Λ_χ^2. As a consequence of this approximation we shall not identify the cut-off used in the regularization of the internal loop, *i.e.* the bosonic loop, with Λ_χ, but rather keep it as an adjustable parameter whose order of magnitude is $\Lambda \sim 2M_Q \sim \Lambda_\chi$.

In what follows we shall use the bosonized ENJL model where, for each vertex, only the lowest order in the derivative expansion will be kept. This approximation allows us to simplify the calculations and preserves chiral invariance.

2 The effective Lagrangian

We restrict ourselves to the $SU(2)_L \times SU(2)_R$ case. The general form for the meson matrices, singlets or triplets under $SU(2)_V$, reads

$$M = \sum_{a=1}^{8} \frac{1}{\sqrt{2}} M_{(a)} \tau^{(a)} + \frac{1}{\sqrt{2}} M_0 \mathbf{1}, \tag{13}$$

where $\tau^{(a)}, a = 1, ..3$ are the Pauli matrices with $Tr(\tau^a \tau^b) = 2\delta^{ab}$ and M_0 is the singlet component. We use for the pseudoscalar field the exponential parametrization $\xi(\Phi) = \exp(-\frac{i}{\sqrt{2}}\frac{\Phi}{f_\pi})$.

In the chiral limit ($m_u = m_d = 0$), the effective chiral Lagrangian including scalar and pseudoscalar mesons to $O(p^2)$ is given by:

$$\begin{aligned}
&\mathcal{L}^{S,P} = \tfrac{f_\pi^2}{4} < \xi_\mu \xi^\mu > + \tfrac{1}{2} < d_\mu S d^\mu S > - \tfrac{1}{2} M_S^2 < S^2 > + \mathcal{L}_{int}^{S,P} \\
&\mathcal{L}_{int}^{S,P} = -\frac{\lambda_3}{3!} < S^3 > - \frac{\lambda_4}{4!} < S^4 > + c_d < S \xi_\mu \xi^\mu > + c_4^{(1)} < S^2 \xi_\mu \xi^\mu > + c_4^{(2)} < S \xi_\mu S \xi^\mu >,
\end{aligned} \tag{14}$$

where S is the scalar meson field and $\xi_\mu = i\{\xi^\dagger(\partial_\mu - i r_\mu)\xi - \xi(\partial_\mu - i l_\mu)\xi^\dagger\}$ is the axial current constructed with the pseudoscalar field, where r_μ and l_μ are the external right-handed and left-handed sources. The couplings among mesons are obtained by integrating out the constituent quark fields in the bosonized ENJL model using the heat kernel expansion with proper time regularization as explained in ref. [2].

[¶] notice however that Z_S differs slightly from the expression given by the heat-kernel calculation; see [4] about this question.

They are functions of the ultra-violet cut-off Λ_χ, the constituent quark mass M_Q, the axial-pseudoscalar mixing parameter g_A and the number of colours N_c. We find:

$$\begin{aligned}
\frac{\lambda_3}{3!} &= \frac{N_c}{16\pi^2} 4 \frac{M_Q}{Z_S^{3/2}} \Big[\Gamma(0,\epsilon) - \frac{2}{3}\Gamma(1,\epsilon) \Big] \\
\frac{\lambda_4}{4!} &= \frac{N_c}{16\pi^2} \frac{1}{Z_S^2} \Big[\Gamma(0,\epsilon) - 4\Gamma(1,\epsilon) + \frac{4}{3}\Gamma(2,\epsilon) \Big] \\
c_d &= \frac{N_c}{16\pi^2} M_Q \frac{2 g_A^2}{\sqrt{Z_S}} \Big[\Gamma(0,\epsilon) - \Gamma(1,\epsilon) \Big] \\
c_4^{(1)} &= \frac{1}{2} \frac{N_c}{16\pi^2} \frac{g_A^2}{Z_S} \Big[\Gamma(0,\epsilon) - \frac{20}{3}\Gamma(1,\epsilon) + \frac{8}{3}\Gamma(2,\epsilon) \Big] \\
c_4^{(2)} &= \frac{1}{2} \frac{N_c}{16\pi^2} \frac{g_A^2}{Z_S} \Big[\Gamma(0,\epsilon) - \frac{10}{3}\Gamma(1,\epsilon) + \frac{4}{3}\Gamma(2,\epsilon) \Big]. \qquad (15)
\end{aligned}$$

The incomplete gamma functions $\Gamma(n-2,\epsilon)$, with $\epsilon = M_Q^2/\Lambda_\chi^2$, are defined as

$$\Gamma(n-2,\epsilon) = \int_\epsilon^\infty \, dz \frac{1}{z} e^{-z} z^{n-2}. \qquad (16)$$

$\Gamma(-2,\epsilon)$ contains a quartic divergence, $\Gamma(-1,\epsilon)$ a quadratic one, $\Gamma(0,\epsilon)$ is logarithmically divergent, while $\Gamma(n,\epsilon)$ with $n > 0$ are finite.

The Interaction Lagrangian of the scalar mesons with vectors and axial-vectors at the first two leading chiral orders, *i.e.* $O(p^0)$ and $O(p^2)$, is[‖]:

$$\begin{aligned}
\mathcal{L}_{int}^{V,A} &= \tilde{c}_A < S A_\mu A^\mu > + c_A^{(1)} < S A_\mu S A^\mu > + c_A^{(2)} < S^2 A_\mu A^\mu > \\
&\quad + c_{AP} < S\{\xi_\mu, A^\mu\} > + c_V^{(1)} < S V_\mu S V^\mu > + c_V^{(2)} < S^2 V_\mu V^\mu > \\
&\quad + \tilde{d}_V < S V_{\mu\nu} V^{\mu\nu} > + d_V^{(1)} < S V_{\mu\nu} S V^{\mu\nu} > + d_V^{(2)} < S^2 V_{\mu\nu} V^{\mu\nu} > \\
&\quad + \tilde{d}_A < S A_{\mu\nu} A^{\mu\nu} > + d_A^{(1)} < S A_{\mu\nu} S A^{\mu\nu} > + d_A^{(2)} < S^2 A_{\mu\nu} A^{\mu\nu} > . \qquad (17)
\end{aligned}$$

Notice also the presence at $O(p^0)$ of the mixed term scalar-pseudoscalar-axial with coupling c_{AP}. Z_V and Z_A are the wave function renormalization constants of the vector and axial-vector fields:

$$Z_V = Z_A = \frac{N_c}{16\pi^2} \frac{1}{3} \Gamma(0,\epsilon) \qquad (18)$$

The couplings are found to be:

[‖] The Lagrangian involving vectors starts at $O(p^2)$. For consistency we need to include $O(p^0)$ as well as $O(p^2)$ terms in the Lagrangian involving axial-vectors.

$$
\begin{aligned}
\tilde{c}_A &= \frac{1}{2}\frac{N_c}{16\pi^2}\frac{M_Q}{\sqrt{Z_S}Z_V}\Big[4\Gamma(0,\epsilon)-4\Gamma(1,\epsilon)\Big] \\
c_A^{(1)} &= \frac{1}{2}\frac{N_c}{16\pi^2}\frac{1}{Z_S Z_V}\Big[\Gamma(0,\epsilon)-\frac{10}{3}\Gamma(1,\epsilon)+\frac{4}{3}\Gamma(2,\epsilon)\Big] \\
c_A^{(2)} &= \frac{1}{2}\frac{N_c}{16\pi^2}\frac{1}{Z_S Z_V}\Big[\Gamma(0,\epsilon)-\frac{20}{3}\Gamma(1,\epsilon)+\frac{8}{3}\Gamma(2,\epsilon)\Big] \\
c_{AP} &= \frac{1}{2}\frac{N_c}{16\pi^2}\frac{g_A M_Q}{\sqrt{Z_S}\sqrt{Z_V}}\Big[-4\Gamma(0,\epsilon)+4\Gamma(1,\epsilon)\Big] \\
c_V^{(1)} &= -c_V^{(2)} = \frac{1}{2}\frac{N_c}{16\pi^2}\frac{1}{Z_S Z_V}\Big[-\Gamma(0,\epsilon)+\frac{2}{3}\Gamma(1,\epsilon)\Big] \\
\tilde{d}_V &= \frac{1}{6}\frac{N_c}{16\pi^2}\frac{1}{M_Q}\frac{1}{\sqrt{Z_S}Z_V}\Gamma(1,\epsilon) \\
\tilde{d}_A &= \frac{N_c}{16\pi^2}\frac{1}{M_Q}\frac{1}{\sqrt{Z_S}Z_V}\Big[\frac{1}{2}\Gamma(1,\epsilon)-\frac{1}{3}\Gamma(2,\epsilon)\Big] \\
d_V^{(1)} &= -\frac{1}{2}\frac{N_c}{16\pi^2}\frac{1}{Z_S Z_V}\frac{1}{M_Q^2}\Big[\frac{1}{6}\Gamma(1,\epsilon)+\frac{2}{15}\Gamma(2,\epsilon)\Big] \\
d_A^{(1)} &= -\frac{1}{2}\frac{N_c}{16\pi^2}\frac{1}{Z_S Z_V}\frac{1}{M_Q^2}\Big[-\frac{1}{6}\Gamma(1,\epsilon)+\frac{7}{15}\Gamma(2,\epsilon)\Big] \\
d_V^{(2)} &= -\frac{1}{2}\frac{N_c}{16\pi^2}\frac{1}{Z_S Z_V}\frac{1}{M_Q^2}\Big[-\frac{1}{3}\Gamma(1,\epsilon)+\frac{1}{5}\Gamma(2,\epsilon)\Big] \\
d_A^{(2)} &= -\frac{1}{2}\frac{N_c}{16\pi^2}\frac{1}{Z_S Z_V}\frac{1}{M_Q^2}\Big[-\frac{1}{3}\Gamma(1,\epsilon)+\frac{23}{15}\Gamma(2,\epsilon)\Big]. \qquad (19)
\end{aligned}
$$

3 Analysis of the $1/N_c$ corrections

In the Appendix we have listed the results for all the loop contributions. We work in the chiral limit ($m_\pi = 0$) and in the zero momentum limit ($q^2 = 0$). The masses of the vector and axial-vector mesons have been fixed to their experimental value: $M_V \simeq 0.770$ GeV [13] and $M_A \simeq 1.2$ GeV (we disregard the error on the axial mass).

We have calculated the $1/N_c$ corrections in two cases: 1) assuming that the scalar particle is a singlet (which, as we said in the introduction, cannot be identified with the $f_0(975)$ resonance) 2) assuming that the quark content of the scalar particle is the same as that of the $\rho(770)$ vector meson. This could be the case of the physical $a_0(983)$ scalar resonance. Obviously our $SU(2)$ calculation has to be interpreted as a first indicative approximation of the fully realistic $SU(3)$ calculation.

The diagrams which contribute to the scalar two-point function at next-to-leading

order in $1/N_c$ are shown in Fig. 2. They are the self-energy (a), the tadpole (b) and the 'top' (c) diagrams.

Particles running in the loop are the singlet and the $SU(2)$ triplet states for each quantum number: Scalar, Pseudoscalar, Vector, and Axial-Vector. We disregard in the present analysis the splitting between the singlet and the triplet pseudoscalar states; this is due to the $U(1)$ axial anomaly, which appears in the effective Lagrangian at next-to-leading order in the $1/N_c$ expansion.

The correction to the mass depends quartically on the UV cut-off Λ of the bosonic loop. It is proportional to

$$\frac{1}{N_c}\left(\frac{\Lambda}{2M_Q}\right)^4. \tag{20}$$

Hence reasonable values of Λ cannot exceed $2M_Q$.

Our conclusions are threefold:

1) The *top* diagram can be alternatively included in the corrections to the scalar propagator or in the gap-equation so that they translate into corrections to the leading-N_c value of M_Q. These corrections do not create any mass splitting between singlet and non-singlet states. In addition they are q^2 independent. The main result concerning these diagrams is the compensation between negative contributions (pseudoscalar and scalar) and positive contributions (vector and axial) so that the corrections to the gap-equation are small.

In Ref. [14] an attempt to compute the $1/N_c$-corrections to the gap equation of the NJL model has been performed in the $G_V = 0$ case. However, the formalism they have adopted implies non-derivative couplings of pseudoscalar mesons to other particles. This makes the comparison with our approach problematic. In particular, the relative size and sign of the scalar and pseudoscalar contributions cannot be compared in the two cases.

2) The mass splitting can arise from the *self-energy* diagrams and the *tadpole* diagrams, but not from the *top* diagrams. Our conclusion is that the $1/N_c$-corrections make the non-singlet heavier than the singlet.

3) Both in the scalar singlet and non singlet cases the corrections are negative and quite sensitive to the value of the UV cut-off. Positive values of the renormalized scalar singlet mass are limited to low values of Λ. We have considered the following ranges for the different parameters:

$$
\begin{aligned}
&250\,\mathrm{MeV} \leq M_Q \leq 350\,\mathrm{MeV} \\
&0.6 \leq g_A \leq 0.8 \\
&900\,\mathrm{MeV} \leq \Lambda_\chi \leq 1100\,\mathrm{MeV} \\
&500\,\mathrm{MeV} \leq \Lambda \leq 2M_Q.
\end{aligned}
\tag{21}
$$

For $M_Q \sim 250$ MeV corrections are big in absolute value (more than 100%). For $M_Q \sim 350$ MeV and $\Lambda \sim 500$ MeV we obtain smaller corrections but the mass splitting is also smaller. With $M_Q = 350$ MeV, $\Lambda_\chi = 900$ MeV, $g_A = 0.7$ and $\Lambda = 500$ MeV we find for the singlet $M_s \simeq 500$ MeV and for the non-singlet $M_{ns} \simeq 560$ MeV.

4 Conclusions

Our work is a first attempt to obtain an order of magnitude as well as the sign of the $1/N_c$ corrections to the mass of the scalar resonance in the framework of the ENJL model. A part from the problem of overlapping divergences, there is a definite way of computing these corrections in the full non-bosonized ENJL model. As explained in Section 1 we have performed the calculations within the bosonized ENJL version.

Our main result is the existence at next-to-leading order in $1/N_c$ of a mass-splitting between singlet and non-singlet states, making the non-singlet heavier.

We find that results are extremely sensitive to the values of the UV cut-off Λ of the bosonic loop. Corrections to the singlet mass are negative. However, contrary to the mass-splitting, the overall shift of the singlet can be affected by corrections coming from higher dimensional fermionic operators. Whereas these corrections are about 30% in the vector sector [15] their importance for the scalar sector is not known.

Acknowledgements

It is a pleasure to thank J. Bijnens for having called our attention to this problem,

for many useful discussions and a careful reading of the manuscript. We also thank J. Gasser, H. Leutwyler, P. Minkowski and R. Petronzio for interesting and stimulating discussions.

The work by CB was supported by the EU Contract Nr. ERBCHRXCT 920026. The work by EP was supported by the EU Contract Nr. ERBCHBGCT 930442.

Appendix

Top diagrams

$$\begin{aligned}
S \qquad & i\frac{\lambda_3^2}{4}\frac{1+3}{16\pi^2}\Gamma(-1,M_S) \\
P \qquad & i\frac{\lambda_3 c_d}{2}\frac{2}{f_\pi^2}\frac{1}{M_S^2}\frac{1+3}{16\pi^2}2(m_\pi^2)^2\Gamma(-2,m_\pi) \\
A\,O(p^0) \qquad & i\frac{\lambda_3\tilde{c}_A}{2}\frac{1+3}{16\pi^2}\frac{M_A^2}{M_S^2}\Big[2\Gamma(-2,M_A)+4\Gamma(-1,M_A)\Big] \\
A(V)\,O(p^2) \qquad & -i\lambda_3\tilde{d}_{A(V)}3\frac{1}{M_S^2}\frac{1+3}{16\pi^2}2M_{A(V)}^4\Gamma(-2,M_{A(V)})
\end{aligned} \tag{22}$$

Contributions are the same for singlet and triplet propagator.

Self-energy diagrams (at $q^2 = 0$)

Singlet propagator

$$\begin{aligned}
S \qquad & i\frac{\lambda_3^2}{4}\frac{1+3}{16\pi^2}\Gamma(0,M_S) \\
P \qquad & ic_d^2\Big(\frac{2}{f_\pi^2}\Big)^2\frac{1+3}{16\pi^2}\Big[2m_\pi^4\Gamma(-2,m_\pi)-m_\pi^4\Gamma(-1,m_\pi)+m_\pi^4\Gamma(0,m_\pi)\Big] \\
A\,O(p^0)\times O(p^0) \qquad & i(\tilde{c}_A)^2\frac{1+3}{16\pi^2}\Big[2\Gamma(-2,M_A)+\Gamma(-1,M_A)+3\Gamma(0,M_A)\Big] \\
A\,O(p^0)\times O(p^2) \qquad & -2i\tilde{c}_A\tilde{d}_A\frac{1+3}{16\pi^2}6M_A^2\Big[\Gamma(-1,M_A)-\Gamma(0,M_A)\Big] \\
A(V)\,O(p^2)\times O(p^2) \qquad & i\tilde{d}_{A(V)}^2\frac{1+3}{16\pi^2}12M_{A(V)}^4\Big[2\Gamma(-2,M_{A(V)})-\Gamma(-1,M_{A(V)})+\Gamma(0,M_{A(V)})\Big] \\
A-P \qquad & 2ic_{AP}^2\frac{2}{f_\pi^2}\frac{1+3}{16\pi^2}\frac{1}{M_A^2}2m_\pi^4\Gamma(-2,m_\pi)
\end{aligned} \tag{23}$$

Triplet propagator

The only possible self-energy diagrams for the triplet propagator contain two differ-

ent internal lines, one singlet and one triplet. The contribution is half the contribution to the singlet propagator displayed above.

Tadpole diagrams

Singlet propagator

$$
\begin{aligned}
S \qquad & -i\frac{\lambda_4}{4}M_S^2\frac{1+3}{16\pi^2}\Gamma(-1,M_S), \\
P \qquad & -i(c_4^{(1)}+c_4^{(2)})\frac{2}{f_\pi^2}\frac{1+3}{16\pi^2}2m_\pi^4\Gamma(-2,m_\pi) \\
A(V)\,O(p^0) \qquad & -i(c_{A(V)}^{(1)}+c_{A(V)}^{(2)})\frac{1+3}{16\pi^2}M_{A(V)}^2\Big[2\Gamma(-2,M_{A(V)})+4\Gamma(-1,M_{A(V)})\Big] \\
A(V)\,O(p^2) \qquad & i(d_{A(V)}^{(1)}+d_{A(V)}^{(2)})6\frac{1+3}{16\pi^2}2M_{A(V)}^4\Gamma(-2,M_{A(V)})
\end{aligned}
\tag{24}
$$

Notice that in the singlet case there are no contributions from vector vertices of order $O(p^0)$ like $< SV_\mu V^\mu >$, because $c_V^{(1)} + c_V^{(2)} = 0$.

Triplet propagator

$$
\begin{aligned}
S \qquad & -i\lambda_4(\frac{1}{4}+\frac{1}{4}+\frac{1}{6})M_S^2\frac{1}{16\pi^2}\Gamma(-1,M_S) \\
P \qquad & -i\frac{2}{f_\pi^2}(3c_4^{(1)}-c_4^{(2)}+c_4^{(1)}+c_4^{(2)})\frac{1}{16\pi^2}2m_\pi^4\Gamma(-2,m_\pi) \\
A(V)\,O(p^0) \qquad & -i(-c_{A(V)}^{(1)}+3c_{A(V)}^{(2)}+c_{A(V)}^{(1)}+c_{A(V)}^{(2)})\frac{M_{A(V)}^2}{16\pi^2}\Big[2\Gamma(-2,M_{A(V)})+4\Gamma(-1,M_{A(V)})\Big] \\
A(V)\,O(p^2) \qquad & i(3d_{A(V)}^{(2)}-d_{A(V)}^{(1)}+d_{A(V)}^{(2)}+d_{A(V)}^{(1)})6\frac{1}{16\pi^2}2M_{A(V)}^4\Gamma(-2,M_{A(V)})
\end{aligned}
\tag{25}
$$

References

[1] J. Bijnens, Nordita Preprint 95/10 N,P;

[2] J. Bijnens, C. Bruno and E. de Rafael, *Nucl. Phys.* **B390** (1993) 501;

[3] J. Prades, Z. Phys. C63 (1994) 491;

[4] J. Bijnens, E. de Rafael and H. Zheng, Z. Phys. **C62** (1994) 437;

[5] M. Svec *et al.*, *Phys. Rev.* **D45** (1992) 55; *Phys. Rev.* **D46** (1992) 949;

[6] A. Bramon and E. Massó, *Phys. Lett.* **93B** (1980) 65;

[7] Achasov, *Z. Phys.* **C41** (1988) 309;

[8] J. Weinstein and N. Isgur, *Phys. Rev.* **D27** (1983) 588;

[9] B. S. Zou and D. V. Bugg, *Phys. Rev.* **D48** (1993) R3948;

[10] D. Morgan and M. R. Pennington, *Phys. Rev.* **D48** (1993) 1185;

[11] N. Tornqvist, hep-ph 9504372, preprint HU-SEFT R 1995-05.

[12] T. Hatsuda, T. Kunihiro *Phys. Rep.* **247** (1994)221;

[13] J. Bijnens and J. Prades, *Z. Phys.* **C64** (1994) 475;

[14] D. Ebert *et al.*, hep-th 9412214, JINR preprint E2-94-488.

[15] E. Pallante and R. Petronzio, *Z. Phys.* **C65** (1995) 487;

FIGURE CAPTIONS

1) Self-energy diagram built by dressing the leading-N_c scalar two-point function with one loop of linear chains of constituent quark bubbles.

2) One loop diagrams which give the next-to-leading in $1/N_c$ contribution to the scalar propagator: (a) the self-energy diagram, (b) the tadpole diagram and (c) the "top" diagram. The solid line is a scalar field, while the dashed line in the loop can be any mesonic field.

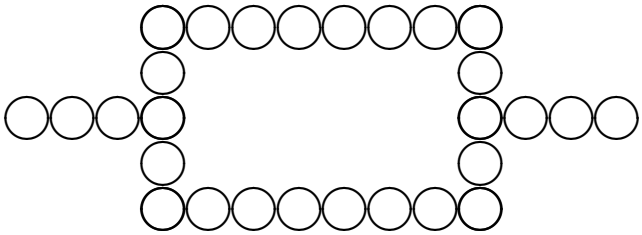

Figure 1:

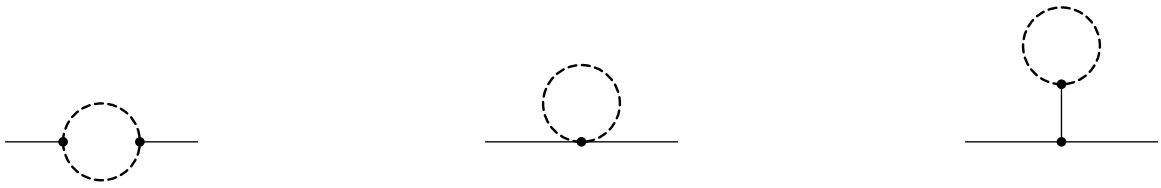

Figure 2: